Working version: Vadym Zayets July 14, 2018

Symmetry and polarity of the voltage-controlled magnetic anisotropy studied by the Anomalous Hall effect

Abstract:

The voltage-controlled magnetic anisotropy (VCMA) effect in FeB, FeCoB and FeB/W films was measured by four independent methods. All measurements are consistent and show the same tendency. In case of the FeB and FeB/W films, the coercive field, Hall angle and anisotropy field linearly decrease when the gate voltage increases. The symmetry and polarity of different mechanisms of the VCMA are analyzed and compared with experimental.

1. Introduction

The VCMA effect describes the fact that in a capacitor, in which one of electrodes is made of a thin ferromagnetic metal, the magnetic properties of the ferromagnetic metal changes, when a voltage is applied to the capacitor. For example, under an applied voltage the magnetization direction of the ferromagnetic metal may be changed[1–3] or even reversed[4,5]. This magnetization-switching mechanism can be used as a data recording method. When an electrical pulse reverses magnetization direction, the data is memorized in the ferromagnetic metal by means of its two opposite magnetization directions. Such a recording mechanism is fast and energy-efficient. It may be used in magnetic the random access memory (MRAM) [6] and the all-metal transistor [7].

Inside a metal the electrical field is screened by free electrons and cannot penetrate deep inside the metal. As a result, the voltage, which is applied to the capacitor dielectric (gate), may penetrate into and affect only the few uppermost atomic layers of the metal near the gate. However, the change of magnetic properties of the uppermost layer by the gate voltage affects the magnetic properties of the whole film. This can be only the case if the interfacial perpendicular magnetic anisotropy (PMA) is affected by the gate voltage.

The interfacial PMA is the effect, which occurs due to a strong spin-orbit (SO) interaction in the upmost atomic layer of the metal[8]. As a result, the magnetic properties of only one upmost atomic layer strongly affect the magnetic properties of the whole film. Since the magnitude of the VCMA effect can be substantial, it is likely that the gate voltage affects the interfacial PMA. However, it is still unclear which particular properties of the upper layer or the whole film are changed by the gate voltage. The interfacial PMA depends on the magnetization of the film, atom arrangement and bonding at the interface. The gate-dependence of each of these properties may be the origin of the VCMA effect. The understanding of the details of the VCMA effect is important in order to optimize and possibly enhance the effect for a future practical application. In this paper we particularly emphasize our study on the symmetry and polarity the VCMA effect with respect to the reversal of the gate voltage. It might be a clue to clarify the origin of the VCMA effect.

There are several methods to measure the VCMA effect. The first conventional method uses a magnetic tunnel junction (MTJ), in which the magnetization of the "reference" layer is in-plane and the magnetization of the "free" layer is perpendicular-to-plane[9,10]. When a magnetic field is applied in the in-plane direction, the magnetization of the "free" layer turns toward the magnetic field. From the measurement of the tunnel resistance, the angle between "free" and "reference" layers is calculated and the PMA energy is estimated. The angle dependence of the tunneling resistance slightly changes under a different voltage applied to the MTJ. It allows to estimate the voltage dependence of the PMA energy. This method assumes that the absolute value of the magnetization is not changed under a gate voltage and that the VCMA does not depend on the magnetization direction. As is shown below, the magnetization is slightly modulated by the gate voltage. Still this method gives a good estimate of the voltage-dependence of the PMA energy. By this method a linear voltage dependency of the PMA energy with a negative slope was measured in Ta:$Fe_{80}Co_{20}B$ [11], Cr:Fe[10], Au:Fe[1], Ru:Co_2FeAl[12] and with a positive slope in Au:$Fe_{80}Co_{20}$ [9]. The negative slope means that the PMA energy increases linearly when the gate voltage

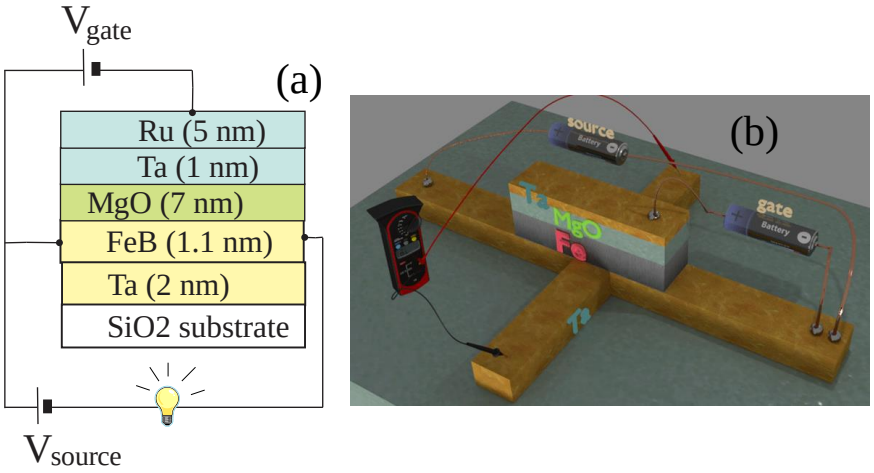

Figure 1. (a) Layer stack of FeB film (b) top-view of measurement setup.

decreases. A symmetric dependence vs the gate-voltage polarity was measured in Cr:Fe:Cr[13]. A $Fe_{84}Co_{16}$ film grown on a Ta buffer shows a negative slope of the VCMA, but the identical film grown on a Ru buffer shows a positive slope [14].

In the second method the voltage dependency of the coercive field is measured. The MTJ, Hall and Kerr configurations were used. A linear voltage dependency of the coercive field with a negative slope was measured in $Ta:Fe_{0.4}Co_{0.4}B_{0.2}$ [15,16], $Au:Fe_{80}Co_{20}$ [3], $Ru:Co_2FeAl$[12] and with a positive slope in Pd:FePd [17], $Ta:Fe_{0.4}Co_{0.4}B_{0.2}$ [18], Pt:Co[19,20]. The third method is the voltage-induced ferromagnetic resonance excitation [21,22]. The explanation of the resonance VCMA effect is more complex and will not be discussed here.

There is some uncertainty in the experimental measurements of the VCMA effect. It is unclear why the polarity of the VCMA is opposite for an identical ferromagnetic film grown on a different buffer [14] and which property makes different the VCMA polarity for nearly identical ferromagnetic metals[15,16,18]. It is unclear whether the voltage-controlled changes of the PMA energy, coercive field and other magnetic parameters are fully correlated. Is a sizeable VCMA is limited only to an ultrathin thin film (thickness< 1 nm)? Or it may be large even in a thicker ferromagnetic metal?

In this work, we have studied the VCMA effect in a FeB/W multilayer and a FeB and $Fe_{0.4}Co_{0.4}B_{0.2}$ films using 4 independent measurements. For each sample, the gate-voltage dependences of the coercive and anisotropy fields, the Hall angle and the magnetization– switching time were measured. The polarity and symmetry of the different possible contributions into the VCMA effect were examined and their correlation with the experimental data is discussed.

2. Experiment

The VCME was measured using the Anomalous Hall effect (AHE)[16,19]. For VCMA measurements, the AHE configuration has several advantages compared to the MTJ configuration. Firstly, there is no undesirable influence of the dipole magnetic field from the reference electrode on measured VCMA properties and there is no undesirable influence of the spin transfer torque due to the flow of the spin-polarized current from the reference electrode. Secondly, different materials of the gate electrode can be tested. The MTJ configuration is limited to a specific ferromagnetic metal, which has to provide a sufficient magneto resistance. There is no such limitation for the Hall configuration. As it is discussed below, a gate material with an optimum work function may be important in order to optimize positon of the Fermi level in a ferromagnetic metal and to increase the VCMA. Thirdly, in the AHE configuration the voltage-dependence of several magnetic parameters can be measured in a single sample (e.g. 4 parameters in this study). Each measurements reveals different features of the VCMA effect.

The samples were fabricated on a Si/SiO2 substrate by sputtering. Figure 1(a) shows a stack of layers. A Ta (2 nm) was used as a buffer layer and a Ta (1 nm)/Ru(5 nm) was used as a gate electrode. A FeB (1.1 nm) or a $Fe_{0.4}Co_{0.4}B_{0.2}$ (1.1 nm) or a FeB(0.8 nm)/W(1.5 nm)/FeB(0.8 nm) multilayer was used as a ferromagnetic layer. A thick MgO (7 nm) layer was used to suppress the tunneling current. A nanowire of different width between 100 and 3000 nm with a Hall probe (Fig.1(b)) was fabricated by the argon milling. The positive gate voltage means that a positive voltage was applied to the non-magnetic electrode.

The change of the coercive field under the gate voltage is not large and it requires a high measurement precision. The estimated precision of our measurements was about 0.9 Oe. A repeated measurement after a 1-month interval is well fit within the precision. The coercive field H_C is the magnetic field, at which the magnetization direction is reversed along its easy axis. The magnetization switching is a thermo-activated process, which is described by the Neel-Brown model[23–25]. The switching time $t_{switching}$ is described by the Arrhenius law as[26]

$$t_{switching} = f^{-1} \cdot e^{\frac{E_{barrier}}{kT}} = f^{-1} \cdot e^{\frac{E_{PMA}}{kT}\left(1-\frac{H}{H_{anis}}\right)^2} \sim t_{retention} \cdot e^{\frac{H \cdot M_{eff}}{kT}} = t_{retention} \cdot e^{\frac{H_C \cdot M_{eff}}{kT}} \quad (1)$$

where $E_{barrier}$ is the energy barrier, which separates two opposite magnetization states; E_{PMA} is the PMA energy; H is the applied perpendicular magnetic field, at which the magnetization is switched; H_{anis} is the anisotropy field; M_{eff} is

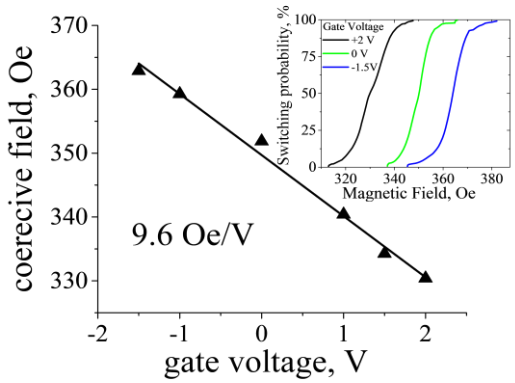

Figure 2 Coercive field vs voltage measured in FeB/W multilayer. Inset shows switching probability from magnetization-up to magnetization-down direction as function of the magnetic field

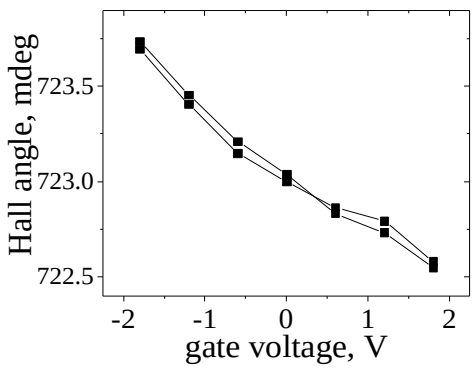

Figure 3. Hall angle as function of the gate voltage in FeB film

the effective magnetization; and $t_{retention}$ is the retention time, which is the average time of magnetization reversal without any external magnetic field.

From Eq.(1), the H_C depends on the measurement time. For example, when measurement time equals to $t_{retention}$, the H_C always equals to zero. Here the measurement time of one second was used for H_C. Due to the dependence of H_C on the measurement time, for a precise measurements of H_C either a sweep magnetic field[27] or a pulsed magnetic field[28] has to be used.

A substantial number of measurements [29] and statistical analysis are required in order to obtain the H_C with a required high precision. In order to shorten the measurement time, we have developed an optimized measurement method of H_C, which consists of two sets of the measurements. In the first measurement, the magnetic pulses of the gradually-increased amplitude was applied and the magnetization switching field was measured. In the second measurement, the magnetic pulses of the constant amplitude was applied and the magnetization switching time was measured. Combining the data from these two measurements, the required measurement precision can be reached faster. The used method is similar to that which was used in Ref. [28]. The details of the optimization of measurements will be described elsewhere.

Figure 2 shows measured H_C of the FeB/W film as the function of the gate voltage. All measurement points fit well to a straight line. The inset of Fig.1 shows the magnetization switching probability at the different gate voltages. The curves practically do not overlap. The change of the coercive field is substantial. It is 9.6 Oe/V. In the case of the FeB sample, the slope is smaller (3.7 Oe/V). The case of the FeCoB film is different, the slope was even smaller (1.9 Oe/V) and the H_c increases at both the negative and the positive gate voltages.

Figure 3 shows the gate-voltage dependency of the Hall angle[30] in the FeB film. In the cases of the FeB and FeB/W films, a straight line with a negative slope fits well all measurement points of the Hall angle. In the case of the FeCoB film we were not able to detect any dependence of the Hall angle on the gate voltage. In the case of the AHE, the Hall angle is proportional to the magnetization of the ferromagnetic metal and the spin polarization of the conduction electrons[31]. It means that the magnetization of the FeB and FeB/W films increases under a negative gate voltage and it decreases under a positive gate voltage. There is a clear relation between the gate-voltage dependencies of the coercive field and the Hall angle (the magnetization)[32].

Figure 4 shows the dependence of the anisotropy field H_{anis} on the gate voltage for the FeB film. The anisotropy field[8,11] is the in-plane magnetic field, at which initially-perpendicular magnetization turns completely into the in-plane direction. The inset of Fig.4 shows the measured in-plane component of the magnetization as a function of the in-plane magnetic field. The slope is substantially different at a different gate voltage. The overcrossing of each line with the x-axis gives the H_{anis}. In the case of the FeB and FeB/W films, the H_{anis} linearly depends on the gate voltage. It increases at a negative gate voltage and decreases at a positive gate voltage. In the case of the FeCoB film, we were not able to detect any gate-voltage dependence of the H_{anis}. There is a clear relation between the gate-voltage dependencies of H_c and H_{anis}. The E_{PMA} can be calculated from the H_{anis} and the saturation magnetization [8,11]. For the FeB film the estimated change of the E_{PMA} is 50 fJ/V m.

Figure 5 shows the dependence of the switching time on the magnitude of an external perpendicular magnetic field. The switching time is still well described by the Arrhenius law (Eq.1) even in the case when magnetic properties are changed by a gate voltage. The switching time becomes longer at a negative gate voltage and shorter at a positive gate voltage. From Eq.(1), the slope of the lines is proportional to M_{eff} and the horizontal offset is proportional to $t_{retention}$ and consequently to E_{PMA}. Data of Fig.5 indicate, that $t_{retention}$ and E_{PMA} substantially depend on the gate voltage. In contrast, the slope is nearly the same. It means that the M_{eff} does not change significantly by the gate voltage. The M_{eff} describes the average bulk magnetization during the magnetization reversal. It is not very sensitive to a small change of magnetization in a small region. In contrast, the Hall angle (Fig.3) is more sensitive to such a small change[31]. Additionally, the measurement of the Hall angle can be done with a higher precision and a

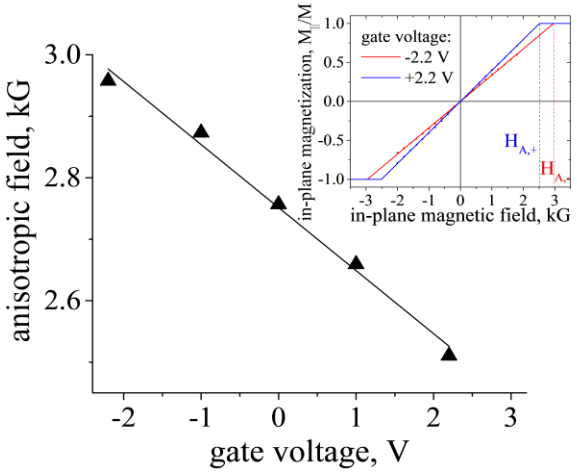

Figure 4. Anisotropic field vs gate voltage in FeB film. Inset shows in-plane magnetization as a function of the in-plane magnetic field. H_{A+}, H_{A-}, are anisotropic fields for V_{gate}= +2.2 V, -2.2 V respectively.

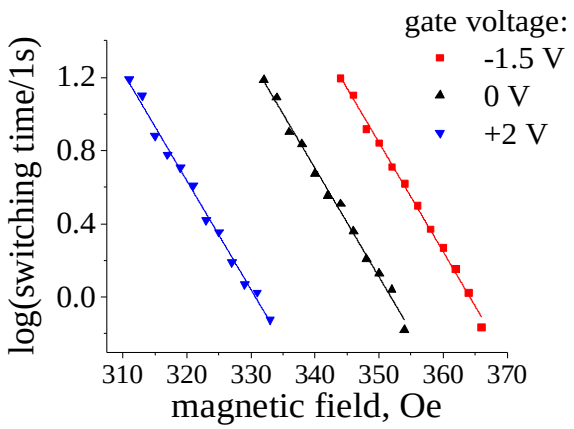

Figure 5. Magnetization switching time in FeB/W multilayer as a function of the perpendicular magnetic field. The line crossing with the x-axis (y=0) gives the coercive field of 363, 351, 330 Oe and the crossing with y-axis (x=0) gives retention time of $10^{21.66}$, $10^{20.88}$, $10^{19.64}$ seconds at V_{gate} = -1.5, 0, +2 V, respectively.

smaller change can be detected. It can be concluded from data of Figs. 3 and 5 that the absolute value of the magnetization are modulated by the gate voltage, but the magnetization change occurs in only a small region in close proximity to the interface.

3. Possible mechanisms of the VCMA effect

The interface PMA occurs due to the strong spin-orbit (SO) interaction in the uppermost atoms of a metal at the gate[8]. The SO interaction is a relativistic effect [33], which states that an electron experiences an effective magnetic field when it moves in a static electrical field. The SO effective magnetic field is proportional to $1/c^2$, therefore it is small. Only in a strong static electrical field, an electron may experience a substantial SO effective magnetic field. In a solid the electrical field is only strong enough in the close proximity of the nucleus in order to induce a substantial SO magnetic field of 1 kGauss or greater. However, in a central-symmetric electrical field of a nucleus the effective SO magnetic field is non-zero only when both the time-inverse symmetry and the spatial symmetry are broken[34]. Otherwise, the effect cancels itself. The intrinsic magnetic field or the magnetization of a ferromagnetic metal breaks the time-inverse symmetry. As a result, the strength of the SO effective magnetic field and the value of the PMA energy are proportional to the magnetization. Our measurements agree well with this fact. The voltage-controlled change of magnetization (Fig.4) is directly related to the change of the PMA energy (Figs.2 and 3).

The second condition for the existing of the SO magnetic field is the breaking of the spatial symmetry. For example, an electron of the s-symmetry, which has the spherical orbital, does not experience any SO interaction, because the spatial symmetry is not broken for such orbital. An external electrical field can break the spatial symmetry. There are several possible orbital deformations, which may lead to the breaking of the spatial symmetry. Firstly, the external electrical field may deform the orbital along its applied direction. Secondly, the electrical field may shift the center of the orbital from center of the nucleus.

The VCMA effect occurs, because an electrical field of the gate changes the degree of the breaking of the time-inverse or/and spatial symmetries. As a result, the strength of the SO interaction and consequently the PMA energy are changed by the electrical field. Based on this fact, several possible origins of the VCMA effect have been discussed. The first mechanism is the modulation of the magnetization by the gate voltage due to the modulation of the Fermi level[16,35]. As was explained above, the modulation of magnetization leads to the modulation of the PMA energy. The screening of an external electrical field by the conduction (delocalized) electrons prevents it from the penetrating deep into the metal. As a result, the conduction electrons are accumulated or depleted in the uppermost layers of a metal. It leads to a change of the Fermi level position in this small region. The magnetization of a ferromagnetic metal depends on the relative amounts of filling of its spin-up and spin-down d-electron states, therefore the value of the magnetization depends on the position of the Fermi level. The result of the gate-voltage modulation of the Fermi level is the modulation of the magnetization and consequently the PMA energy.

A simplified explanation of the polarity of this mechanism can be given as follows. A non-zero magnetization of a ferromagnetic metals means that there are more spin-up localized d-electrons than spin-down d-electrons. As a consequence, there are more unfilled spin-down d-states than unfilled spin-up d-states. Under a positive gate voltage there is an electron accumulation and the Fermi level rises up. This results in the filling of more spin-down than spin-up states. Consequently, the magnetization decreases. Therefore, in this case the VCMA polarity is negative, which was observed in our experiments (Figs. 2-4).

The second possible mechanism of the VCMA effect is the modulation of the spatial symmetry of localized d-electrons by the modulation of the Fermi level [36]. This mechanism is similar to the mechanism of the modulation of the SO interaction of the conduction electrons in a semiconductor [37], which occurs due to the mixing between bands of p- and s- symmetry. A conduction electron, whose energy is at the bottom of the conduction band, has s-symmetry and does not experience any SO interaction. A conduction electron of a higher energy has a component of the p-symmetry and does experiences the SO interaction. By a modulation of the Fermi level, the strength of the SO interaction can be modulated. A similar mechanism was suggested[36] for the localized electrons in a ferromagnetic metal. As a result of a shift of the Fermi level, the spatial symmetry of the localized electrons changes. This leads to the modulation of the strength of the SO interaction and the PMA. The contribution of this mechanism to the VCMA may be substantial only in the case when there are at least two types of states for localized electrons of substantially-different spatial symmetry. However, it is accepted that in bcc Fe only d-electrons of the e_g symmetry are localized [38,39] and there are no localized states of a substantially different symmetry. As a result, a substantial contribution of this mechanism to the VCMA is not expected. It should be noted that the hybridization of the localized d-electrons with p-electrons at the gate interface [40,41]may increase the diversity of the spatial symmetry of the localized electrons and therefore increase the contribution of this mechanism.

The density of states (DOS) in a metal is large. For example, in Fe it is about 1state/eV/atom [42]. In contrast, the number of accumulated/depleted electrons is not as large. For example, it is about 7.7 cm^{-3} under gate voltage of 1 V in the structure of Fig.1. It is questionable whether this relatively-small amount of accumulation may change the position of the Fermi level sufficiently. It depends on how thin is the region of charge accumulation in a metal. In contrast to a semiconductor, which may be fully depleted and in which the region of charge accumulation may be thick, a metal cannot be depleted and the region of charge accumulation in a metal is thin. However it is not infinitely thin. It could be suggested that is about the size of an electron or about the mean-free path [43,44]. The thinner the region of the charge accumulation is in a metal, the larger the change of the Fermi level is at a fixed gate

voltage. For example, if we assume the thickness of the accumulated region to be 0.2 nm, then the change of the Fermi level under 1 V of the gate voltage (Fig.1) would be only 4.5 meV. It is doubtful that the symmetry of localized electrons may substantially be changed due to such a small change of the Fermi energy[45].

In the following we will discuss two possible mechanisms of the VCMA effect, which do not require a change of the Fermi level. The third possible mechanism of the VCMA effect is the modulation of the PMA by the strains[46]. Under a gate voltage, the gate is compressed. Since the electrical field slightly penetrates into a metal, a few uppermost layers of the metal may be compressed as well. Due to the compressive strains the electron orbital is deformed, which may modulate the SO and the PMA. The gate voltage of both polarities equally compresses the gate. As a result, the VCMA induced by the strains should not depend on the polarity of the gate voltage. The measured polarity of the VCMA (Figs.2-4) is opposite for the opposite gate voltages. It can be concluded that the strain-induced mechanism is a minor contributor to the VCMA effect in the studied samples.

The fourth possible mechanism of the VCMA effect is the modulation of the PMA due to an orbital deformation in an electric field [47,48]. The deformation of the orbital induces an electrical dipole moment. Due to this induced dipole moment, the permittivity of a metal ε_{metal} becomes different from the vacuum permittivity ε_0. As was mentioned above, the deformation of the orbital enhances the SO interaction. The larger the ε_{metal}, is, the larger the orbital deformation is and as a consequence the larger the SO enhancement becomes. The polarity of this contribution can be both symmetrical and asymmetrical with respect to the polarity of the gate voltage. The schematic diagrams in Fig.5 illustrate both the symmetrical ((a)-(c)) and the asymmetrical ((d)-(e)) contributions. In the case of a centrosymmetric orbital in the absence of an external electrical field, there are neither a net electrical dipole moment $\boldsymbol{P}$ nor an effective SO magnetic field $\boldsymbol{H_{SO}}$ (Fig.5a). In an electrical field, the electron orbital and the nucleus are slightly shifted relatively to each other and the electrical dipole moment $\boldsymbol{P}$ is induced. The breaking of the spatial symmetry along the $\boldsymbol{M}$ direction induces $\boldsymbol{H_{SO}}$ (Fig.5(b,c)). The polarity of $\boldsymbol{H_{SO}}$ does not depend on the polarity of the electrical field. It is always directed along $\boldsymbol{M}$. As a result, the change of $\boldsymbol{H_{SO}}$ and correspondently the PMA energy do not depend on the polarity of the gate voltage. The case of an elliptical orbital is different. For example, the electron orbital may be elongated toward the gate due to an attraction of an oxygen atom. In this case, the $\boldsymbol{P}$ and $\boldsymbol{H_{SO}}$ are non-zero even in the absence of an external electrical field (Fig.5d). An electrical field either reduces or enhances $\boldsymbol{P}$ and $\boldsymbol{H_{SO}}$ (Figs. 5(e,f) depending on its polarity. Even though the $\boldsymbol{H_{SO}}$ does not reverse its own direction, the changes of $\boldsymbol{H_{SO}}$ are opposite for the opposite polarities of the gate voltage. As shown in Figs. 5(e,f), the $\boldsymbol{H_{SO}}$ and correspondently the PMA energy are larger under a positive gate voltage and smaller under a negative gate voltage. This predicted polarity of VCME is opposite to the polarity of our measurements (Figs. 2-4). In the case when the orbital deformation could be opposite to that shown in Fig.5d, the VCME polarity would be the same as in our experiment.

As was mentioned above, only the regions with the highest electrical field contribute substantially to the SO effective magnetic field. As a result, the region of close proximity to the nucleus (Fig.5) is mostly important to determine the strength of the SO interaction. This is the reason why the simplified description of Fig.5 is valid for the electrons of p- and d-symmetries as well.

It should be noted that an electrical field penetrates into the metal only within the region of the charge accumulation. It is largest at the gate interface and it vanishes at the boundary of the accumulation region. As a consequence, only the uppermost atoms of Fe may experience a substantial dipole-type VCMA.

The ionic diffusion under a gate voltage following the reversible electrochemical reaction [49,50] is another mechanism of the VCMA. It is a slow mechanism having a hysteretic response, which was not observed in the studied samples.

4. Discussion

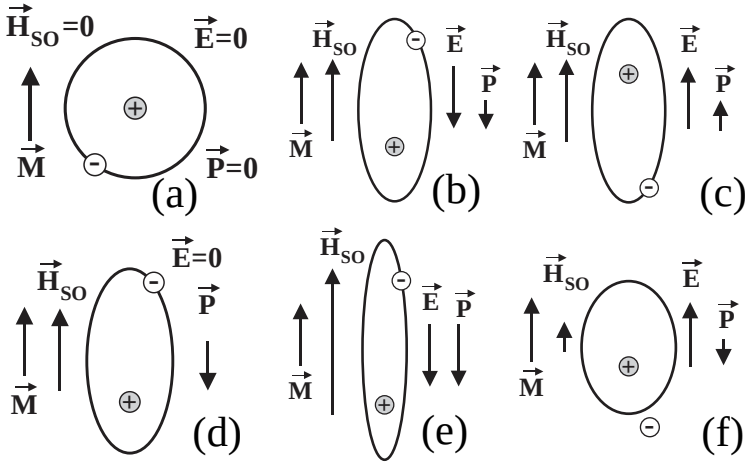

Fig.6. Deformation of electron orbital under a gate voltage. Ellipses show lines of constant electron density in the close proximity of the nuclear. (a),(d) $V_g=0$; (b),(e) $V_g>0$; (c),(f) $V_g<0$. Without gate voltage, the orbit is (a)-(c) centrosymmetric; (d)-(f) elongated toward the gate. The gate location is under orbital. **P** is the net electrical polarization, **M** is the magnetization and $\mathbf{H_{SO}}$ is the effective magnetic field of SO interaction.

It is likely that main mechanism of the VCMA in our studied samples (FeB and FeB/W films) is the voltage-controlled change of the magnetization due to a change of the Fermi level. This mechanism explains well the polarity of the experimentally-measured VCMA effect. Additionally, the VCMA polarity is well matched to the measured polarity of the magnetization change. The estimation of the relatively-small change of the Fermi level by the gate voltage creates some doubt about the domination of this mechanism. The above estimation of the Fermi level change may be underestimated. Additional factors might have a substantial influence. For example, the surface states [51] might be the main electronic states at the gate interface. The DOS of the surface states is significantly smaller than the DOS of the conduction electrons in the bulk of a metal[51]. It would make the change of the Fermi level significantly larger. Only an experimental measurement may clarify the actual value of the change.

The magnetization-modulation mechanism can be enhanced in the case of a presence of a sharp peak in the DOS of a ferromagnetic metal near the Fermi level. This fact can be explained as follows. The magnetization change *dM* under a gate voltage can be calculate as

$$dM = \frac{\partial M}{\partial E} \cdot dE_{Fermi} \qquad (2)$$

where dE_{Fermi} is the change of the Fermi level, *M(E)* is the dependence of the magnetization on the Fermi level. The $\frac{\partial M}{\partial E}$ is larger, when the DOS of the localized electrons has a greater slope near the Fermi level. Ab-initial calculations predict that there is a sharp peak [39,42] in the DOS of the localized e_g -electrons in iron. Our experimental data is well matched to the prediction for the existence of the peak. For example, the Fermi level might be near a slope of this peak in the cases of the FeB and FeB/W samples. As a result, the VCMA in these samples is large. In contrast, the VCME in the FeCoB sample is small, because its Fermi level is either at the top peak or far from the peak.

Some additional experimental facts can be well explained by the magnetization-modulation mechanism as well. As was mentioned above, the polarity and the strength of the VCMA depends significantly on the material of a buffer layer under the ferromagnetic metal. This is puzzling because the electrical field cannot penetrate deep into a metal and cannot reach the buffer. However, it was experimentally found that a Cr buffer enhances the VCMA [10] and the replacement of the Ta buffer with the Ru buffer changes the sign of the VCMA effect[14]. It can be explained as follows[32]. When two metals of different work functions (WF) are in contact, some electrons move from one metal to another in order to equalize the Fermi level. As a result, the Fermi level changes in a thin region of the charge accumulation near the metal contact. When the buffer layer is close enough to the gate, this region can be extended up to the gate interface and it can influence the Fermi level there. The WFs of Fe,Cr and W are nearly equal[52]. Therefore, the Cr or W buffer may slightly turn the Fermi level to the greatest slope of *M(E)* making the VCMA larger. The WF of Ta is 250 meV smaller than that of Fe and the Fermi level in Fe on a Ta buffer rises up out of the slope. As a result, the VCME decreases. The WF of Ru[52] is 210 meV greater than that of Fe and the Fermi level in Fe on a Ru buffer falls down and it may move from the higher-energy negative slope of the peak of *M(E)* to the lower-energy positive slope of the peak. As a result, the polarity of the VCME may change from negative to positive when a Ru buffer is used[53].

The gate electrode is closer to the gate/ferromagnetic-metal interface than the buffer. As a result, an electrode material may have greater influence on the Fermi level at the interface than a material of the buffer. A systematical study of the VCMA dependence on the work function of the gate electrode might clarify the contribution of this mechanism to the VCMA.

One argument against the domination of the magnetization-modulation mechanism is that a peak-like feature has not been observed in the voltage dependence of the tunnel resistance (TR) and TMR[54]. It might indicate that there is no peak near the Fermi level in DOS of Fe or the peak is broad[39,42]. Still even a broad peak may give a sufficient enhancement of the VCMA. It should be noted that TR and TMR are influenced mainly by properties of the conduction (delocalized) electrons[55], but a peak in DOS was predicted for localized e_g -electrons [39,42].

5. Conclusions

The gate-voltage dependence of the magnetization switching time, Hall angle, anisotropic and coercive fields have been studied in the FeB/W, FeB and $Fe_{0.4}Co_{0.4}B_{0.2}$ films. The gate-voltage dependences of all these values are clearly related. In the FeB/W and FeB films, all 4 values linearly increase with the decrease of the gate voltage. The dependence is asymmetric with respect to the reversal of the gate voltage. In the $Fe_{0.4}Co_{0.4}B_{0.2}$ film, the VCMA is significantly smaller and the voltage dependence is nearly symmetric.

The polarity and symmetry of the different possible mechanisms of the VCMA effect were examined. The slope and polarity of measured data imply that a change of the Fermi level, which leads to the corresponded changes of the magnetization and the PMA energy, may be a major contributor to the VCMA effect. Additionally, the detected magnetization change under a gate voltage supports this suggestion.

The VCMA effect is found to be substantially larger in the FeB/W multilayer than in a FeB thin film. This demonstrates that the VCMA effect is not limited by an ultrathin film (thickness <1 nm) and the VCMA may be a substantial even in a thicker film.

References

[1] T. Maruyama, Y. Shiota, T. Nozaki, K. Ohta, N. Toda, M. Mizuguchi, A.A. Tulapurkar, T. Shinjo, M. Shiraishi, S. Mizukami, Y. Ando, Y. Suzuki, Nat. Nanotechnol. 4 (2009) 158–161.

[2] M. Weisheit, S. Fähler, A. Marty, Y. Souche, C. Poinsignon, D. Givord, 315 (2007).

[3] Y. Shiota, T. Maruyama, T. Nozaki, T. Shinjo, M. Shiraishi, Y. Suzuki, Appl. Phys. Express 2 (2009) 8–11.

[4] Y. Shiota, S. Miwa, T. Nozaki, F. Bonell, N. Mizuochi, T. Shinjo, H. Kubota, S. Yuasa, Y. Suzuki, Appl. Phys. Lett. 101 (2012) 102406.

[5] Y. Shiota, T. Nozaki, F. Bonell, S. Murakami, T. Shinjo, Y. Suzuki, Nat. Mater. 11 (2012) 39–43.

[6] Y. Shiota, T. Nozaki, S. Tamaru, K. Yakushiji, H. Kubota, A. Fukushima, S. Yuasa, Y. Suzuki, Appl. Phys. Express 9 (2016).

[7] V. Zayets, T. Nozaki, A. Fukushima, S. Yuasa, All-Metal Transistor and Its Operational Method, 2017–226503, 2017.

[8] M.T. Johnson, P.J.H. Blomen, F.J.A. den Broeder, J.J. de Vries, Reports Prog. Phys. 59 (1996) 1409.

[9] Y. Shiota, S. Murakami, F. Bonell, T. Nozaki, T. Shinjo, Y. Suzuki, Appl. Phys. Express 4 (2011) 043005.

[10] T. Nozaki, A. Kozioł-Rachwał, W. Skowroński, V. Zayets, Y. Shiota, S. Tamaru, H. Kubota, A. Fukushima, S. Yuasa, Y. Suzuki, Phys. Rev. Appl. 5 (2016).

[11] J.G. Alzate, P. Khalili Amiri, G. Yu, P. Upadhyaya, J.A. Katine, J. Langer, B. Ocker, I.N. Krivorotov, K.L. Wang, Appl. Phys. Lett. 104 (2014).

[12] Z. Wen, H. Sukegawa, T. Seki, T. Kubota, K. Takanashi, S. Mitani, Sci. Rep. 7 (2017) 45026.

[13] A. Kozioł-Rachwał, T. Nozaki, K. Freindl, J. Korecki, S. Yuasa, Y. Suzuki, Sci. Rep. 7 (2017) 1–3.

[14] Y. Shiota, F. Bonell, S. Miwa, N. Mizuochi, T. Shinjo, Y. Suzuki, Appl. Phys. Lett. 103 (2013).

[15] W.G. Wang, M. Li, S. Hageman, C.L. Chien, Nat. Mater. 11 (2012) 64–68.

[16] M. Endo, S. Kanai, S. Ikeda, F. Matsukura, H. Ohno, Appl. Phys. Lett. 96 (2010) 10–13.

[17] F. Bonell, S. Murakami, Y. Shiota, T. Nozaki, T. Shinjo, Y. Suzuki, Appl. Phys. Lett. 98 (2011) 96–99.

[18] H. Meng, V.B. Naik, R. Liu, G. Han, Appl. Phys. Lett. 105 (2014) 042410.

[19] D. Chiba, S. Fukami, K. Shimamura, N. Ishiwata, K. Kobayashi, T. Ono, Nat. Mater. 10 (2011) 853–856.

[20] S. Nakazawa, A. Obinata, D. Chiba, K. Ueno, Appl. Phys. Lett. 110 (2017).

[21] T. Nozaki, Y. Shiota, M. Shiraishi, T. Shinjo, Y. Suzuki, Appl. Phys. Lett. 96 (2010).

[22] A. Okada, S. Kanai, M. Yamanouchi, S. Ikeda, F. Matsukura, H. Ohno, Appl. Phys. Lett. 105 (2014) 1–5.

[23] W.F. Brown, Phys. Rev. 130 (1963) 1677–1686.

[24] L. Néel, Adv. Phys. 4 (1955) 191–243.

[25] W.T. Coffey, Y.P. Kalmykov, J. Appl. Phys. 112 (2012).

[26] Comment1, (n.d.).

[27] X. Feng, P.B. Visscher, in: J. Appl. Phys., 2004, pp. 7043–7045.

[28] W. Wernsdorfer, Adv. Chem. Phys. 44 (2001) 217.

[29] L. Tillie, E. Nowak, R.C. Sousa, M.C. Cyrille, B. Delaet, T. Magis, A. Persico, J. Langer, B. Ocker, I.L. Prejbeanu, L. Perniola, Tech. Dig. - Int. Electron Devices Meet. IEDM (2017) 27.3.1-27.3.4.

[30] Comment2, (n.d.).

[31] C.M. Hurd, The Hall Effect in Metals and Alloys, Plenum Press, 1972.

[32] Comment3, (n.d.).

[33] L.D. (Lev D. Landau, E.M. (Evgeniĭ M. Lifshits, The Classical Theory of Fields, 4th rev. E, Pergamon Press, 1975.

[34] P. Bruno, Phys. Rev. B 39 (1989) 865–868.

[35] K. Yamada, H. Kakizakai, K. Shimamura, M. Kawaguchi, S. Fukami, N. Ishiwata, D. Chiba, T. Ono, Appl. Phys. Express 6 (2013) 8–11.

[36] C.G. Duan, J.P. Velev, R.F. Sabirianov, Z. Zhu, J. Chu, S.S. Jaswal, E.Y. Tsymbal, Phys. Rev. Lett. 101 (2008) 1–4.

[37] J.M. Luttinger, W. Kohn, Phys. Rev. 97 (1955) 869–883.

[38] J.B. Goodenough, Phys. Rev. 120 (1960) 67–83.

[39] A.A. Katanin, A.I. Poteryaev, A. V. Efremov, A.O. Shorikov, S.L. Skornyakov, M.A. Korotin, V.I. Anisimov, Phys. Rev. B - Condens. Matter Mater. Phys. 81 (2010) 1–8.

[40] J. Okabayashi, J.W. Koo, H. Sukegawa, S. Mitani, Y. Takagi, T. Yokoyama, Appl. Phys. Lett. 105 (2014).

[41] H.X. Yang, M. Chshiev, B. Dieny, J.H. Lee, A. Manchon, K.H. Shin, Phys. Rev. B - Condens. Matter Mater. Phys. 84 (2011) 1–5.

[42] J. Zhang, P. V. Lukashev, S.S. Jaswal, E.Y. Tsymbal, Phys. Rev. B 96 (2017) 1–8.

[43] V. Zayets, J. Magn. Magn. Mater. 445 (2018).

[44] V. Zayets, J. Magn. Magn. Mater. 356 (2014) 52–67.

[45] Comment4, (n.d.).

[46] P. V. Ong, N. Kioussis, D. Odkhuu, P. Khalili Amiri, K.L. Wang, G.P. Carman, Phys. Rev. B - Condens. Matter Mater. Phys. 92 (2015) 1–5.

[47] K. Nakamura, R. Shimabukuro, T. Akiyama, T. Ito, A.J. Freeman, Phys. Rev. B 80 (2009) 172402.

[48] F. Ibrahim, H.X. Yang, A. Hallal, B. Dieny, M. Chshiev, Phys. Rev. B 93 (2016).

[49] C. Bi, Y. Liu, T. Newhouse-Illige, M. Xu, M. Rosales, J.W. Freeland, O. Mryasov, S. Zhang, S.G.E. te Velthuis, W.G. Wang, Phys. Rev. Lett. 113 (2014) 267202.

[50] U. Bauer, L. Yao, A.J. Tan, P. Agrawal, S. Emori, H.L. Tuller, S. van Dijken, G.S.D. Beach, Nat. Mater. 14 (2015) 174–181.

[51] S.M. Sze, K.K. Ng, Physics of Semiconductor Devices, 3rd ed., Wiley-Interscience, 2007.

[52] H.B. Michaelson, J. Appl. Phys. 48 (1977) 4729–4733.

[53] Comment5, (n.d.).

[54] S. Yuasa, T. Nagahama, A. Fukushima, Y. Suzuki, K. Ando, Nat. Mater. 3 (2004) 868–871.

[55] C. Kaiser, A.F. Panchula, S.S.P. Parkin, Phys. Rev. Lett. 95 (2005) 047202.

[56] R.H. Victora, Phys. Rev. Lett. 63 (1989) 457–460.

Comment1:

The barrier $E_{barrier}$ is equal to $E_{barrier} = E_{anis,\perp}\left(1-\frac{H}{H_{anis}}\right)^{m}$. In the original Neel paper[24], m=2 was calculated from the barrier height. Later[56] it was found that m=3/2 is a better fit to the experimental data and therefore it was conventionally used. However, in case of the uniaxial anisotropy and when the magnetic field applied perpendicularly to the film, m=2 is still a better fit for experimental data[28]. Here, m=2 was used. In the case when $\frac{H}{H_{anis}} \ll 1$, the barrier height can be approximated as $E_{barrier} \approx E_{anis,\perp}\left(1-2\frac{H}{H_{anis}}\right) = E_{anis,\perp} - H \cdot M_{eff}$. For all our studied samples $\frac{H_C}{H_{anis}} \approx 2\%$, and all measurements were done in the close vicinity of H_C.

Comment2:

The Hall angle is linearly proportional to the Hall resistance. In contrast to the Hall resistance, the Hall angle[31] is only material dependent and does not depend on a film thickness.

Comment 3

The voltage-dependence of magnetization with a positive slope was measured in Pt/Co film [35]. It is well correlated with a positive slope of the voltage-dependence of coercive field in a similar sample [19]

Comment4:

Sometimes this effect is called the “hole” or the “electron” doping [42]. It should be noted that the ratio of electrons and holes in a metal is nearly equal [43] and it may change only slightly, when the Fermi level is changed.

Comment 5:

Another mechanism might be responsible for the opposite polarities of the VCMA effect in FeB grown on a Ru and Ta buffer. The FeB might preferentially have recrystallized into the bcc phase on the Ta buffer and into the FCC phase on the Ru buffer.

Figure captions

Figure 1. (a) Layer stack of FeB film (b) top-view of measurement setup.

Figure 2 Coercive field vs voltage measured in FeB/W multilayer. Inset shows switching probability from magnetization-up to magnetization-down direction as function of the magnetic field

Figure 3. Hall angle as function of the gate voltage in FeB film

Figure 4. Anisotropic field vs gate voltage in FeB film. Inset shows in-plane magnetization as a function of the in-plane magnetic field. H_{A+}, H_{A-}, are anisotropic fields for V_{gate}= +2.2 V , -2.2V respectively.

Figure 5. Magnetization switching time in FeB/W multilayer as a function of the perpendicular magnetic field. The line crossing with the x-axis (y=0) gives the coercive field of 363, 351, 330 Oe and the crossing with y-axis (x=0) gives retention time of $10^{21.66}$, $10^{20.88}$, $10^{19.64}$ seconds at V_{gate} = -1.5, 0, +2 V, respectively.